Rev. Adv. Mater. Sci. 43 (2015) 89-93

LOCAL CRYSTAL-TO-GLASS AND GLASS-TO-CRYSTAL TRANSFORMATIONS IN GRAPHENE UNDER TENSILE DEFORMATION

A.S. Kochnev[1] and I. A. Ovid'ko[1,2,3]

[1]Department of Mathematics and Mechanics, St. Petersburg State University, St. Petersburg 198504, Russia
[2]Research Laboratory for Mechanics of New Nanomaterials,
Peter the Great St. Petersburg Polytechnic University, St. Petersburg 195251, Russia
[3]Institute of Problems of Mechanical Engineering, Russian Academy of Sciences,
St. Petersburg 199178, Russia

Received: October 29, 2015

Abstract. Deformation processes and structural transformations in graphene containing 5-8-5 defects - divacancies associated with "pentagon-octagon-pentagon" configurations of carbon atoms - are simulated by molecular dynamics method exploiting the adaptive intermolecular reactive bond order (AIREBO) potential. These computer simulations have shown that both crystal-to-glass and reverse glass-to-crystal transformations occur in a nanoscale region (at a pre-existent 5-8-5 defect) of graphene under tensile deformation at temperature of 2300K.

1. INTRODUCTION

Graphene specified by the outstanding electronic, thermal, energy-storage and mechanical properties represents the subject of intensive research efforts; see, e.g., reviews [1-10]. These efforts are motivated by a huge potential of functional and structural applications of both graphene materials and composites containing graphene inclusions [1-15]. The remarkable properties of graphene are highly sensitive to their hexagonal crystalline structure and presence of crystal-lattice defects [16-19]. In some circumstances, initially crystalline graphene under irradiation treatment transforms into its amorphous counterpart showing the specific characteristics [20-23]. Crystal-to-glass transformations induced by irradiation occurs through generation of multiple vacancies associated with various configurations of 5, 7- and 8-cells as well as large *n*-cells (*n*-membered rings of carbon atoms) with $n > 8$ [20-23]. These defects form glassy graphene nuclei growing with irradiation treatment time.

Irradiation-induced crystal-to-glass transformations in 2D graphene serve as analogs of such transformations occurring in conventional 3D crystalline solids under irradiation; see, e.g., [24,25] and references therein. At the same time, in 3D solids, crystal-to-glass transformations can be induced by mechanical load [26-28], but not only irradiation. Besides, amorphous 3D solids under thermal treatment and mechanical load can undergo glass-to-crystal transformations resulting in formation of (nano)crystalline structure; see, e.g., [29,30] and references therein. In the context discussed, it is highly interesting to understand, if stress-induced crystal-to-glass and glass-to-crystal transformations can come into play in mechanically loaded graphene whose properties can be controlled by such transformations. The main aim of this paper is to present results of molecular dynamics (MD) simulations showing both crystal-to-glass and reverse glass-to-crystal transformations occurring in a nanoscale region of a mechanically loaded graphene initially (before deformation) containing a 5-8-5 defect.

Corresponding author: I.A. Ovid'ko, e-mail: ovidko@nano.ipme.com

2. SIMULATION METHOD

In description of structural transformations in mechanically loaded graphene containing 5-8-5 defects, we exploited the Large-scale Atomic/Molecular Massively Parallel Simulator MD simulation package. In order to specify interatomic bonds, we used the AIREBO potential [31] which is conventionally utilized in computer models of mechanically loaded graphene structures. More details of the computational procedure can be found in Ref. [32]. In this section, we briefly discuss the specific features of our simulations focused on structural transformations in graphene sheets containing 5-8-5 defects in the exemplary situation where such defects have long axes making a 60° angle with the tension load (Fig. 1).

In our simulations with the AIREBO potential, the cut-off radius specifying short-range covalent interactions is chosen as 2.0 Å. This value of the cut-off radius is exploited, because of its good correspondence to characteristics of real graphene [33].

In order to describe tension tests of graphene sheets, the simulation cells are used with periodic boundary conditions along x and y directions (in the Cartesian coordinate system shown in Fig. 1) The sizes of the simulation cell are chosen as 3.5 nm and 3.5 nm, and the cell contains 446 carbon atoms (Fig. 1). As it has been demonstrated in Ref. [34], such sizes of the simulation cell are large enough for effective approximate description of deformation and fracture processes in graphene. The distance between carbon atoms in graphene in its initial (pre-deformation) state is used to be 1.42 Å; see review [6] and references therein. The graphene sheet thickness is taken as 3 Å.

The simulations were performed at high temperature (2300K) at which structural transformations are enhanced in graphene. The tensile strain was applied in the y direction (in the Cartesian coordinate system shown in Fig. 1) with a strain rate of 0.005 $fsec^{-1}$. The simulation step in time is chosen as 1 femptosecond.

3. RESULTS AND DISCUSSION

Our simulations of tensile deformation test for a free-standing graphene sheet with a 5-8-5 defect at temperature of 2300K have shown that deformation processes occur in the sheet through both transformations of the defect and associated nanoscale amorphization, that is, crystal-to-glass transformation (Figs. 2a-2e). More precisely, at the first tension stage (Figs. 2a and 2b), the initial 5-8-5 defect transforms into a local region with disorderedly ar-

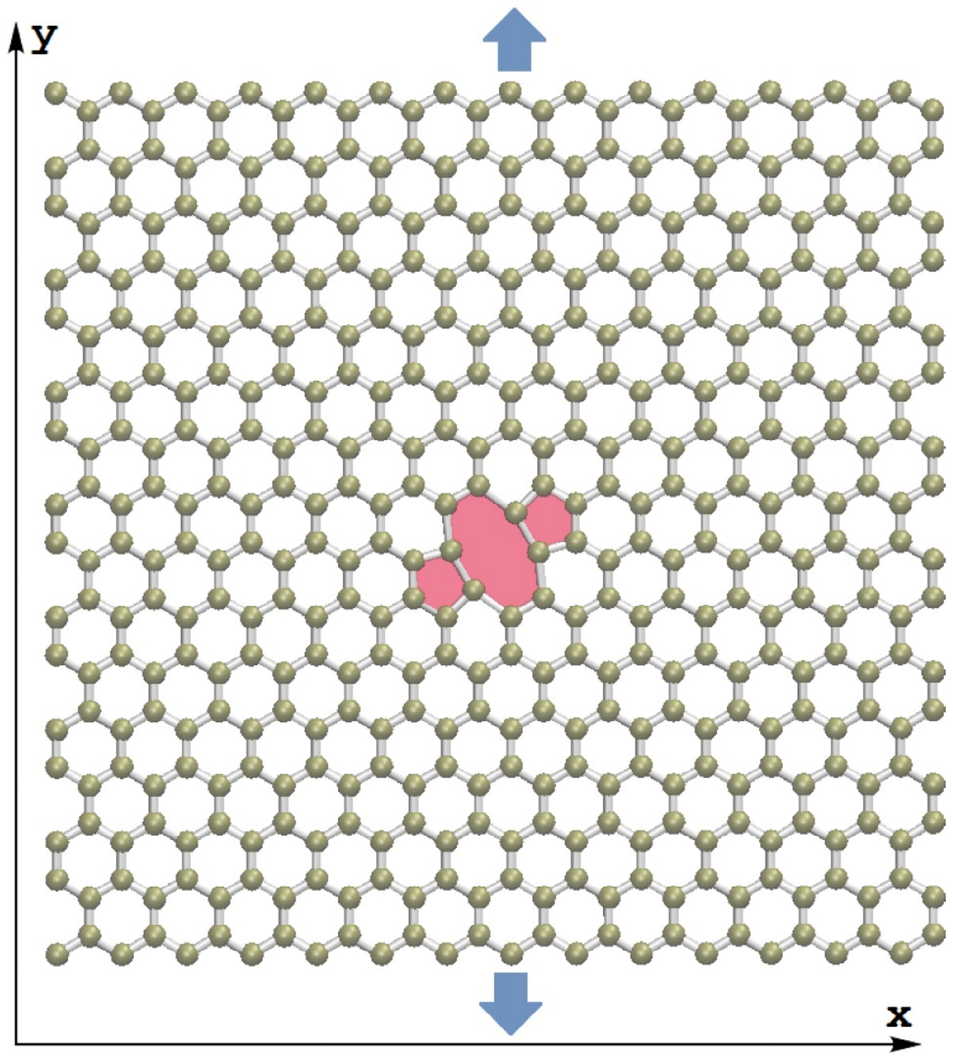

Fig. 1. (Color online) Graphene sheet contains a 5-8-5 defect (pink colored configuration consisting of two 5-cells and a 8-cell of carbon atoms). Tensile load of graphene sheet is directed along *y* axis of the coordinate system shown in Figure.

ranged carbon atoms at and near the initial position of the defect. Sizes of the region are of around 1 nm. The local disordered region consists of *n*-cells (*n*-membered rings of carbon atoms) with $n \neq 6$, in which case *n*-cells with $n > 6$ dominate over those characterized by $n < 6$. In particular, there are three and two large *n*-cells with $n \geq 10$ in the graphene sheet at strain of $\varepsilon = 0.5$ and 1%, respectively (Figs. 2a and 2b, respectively). Formation of such large cells involves breaks of interatomic C-C bonds. In spirit of definition/description [20-23] (based on computer simulations and experimental data) of irradiation-produced amorphous graphene, the local disordered region under discussion is logically treated as a nanoscale inclusion of amorphous graphene in a crystalline graphene matrix.

With further increase in strain up to values of ε = 1.5, 2, and 2.5% (Figs. 2c, 2d, and 2e, respectively), the amorphous graphene region undergoes some structural transformations keeping its atomic arrangement as disordered one. In doing so, its sizes become smaller, and the number of *n*-cells with $n < 6$ increases, although large *n*-cells with $n > 6$ still exist and evolve. Also, new dislocations (pairs of 5- and 7-cells) are generated in the amorphous graphene region at ε = 1.5% (Fig. 2c). On the one hand, this process resembles processes of dislocation generation at the intergranular amorphous phase in 3D nanoceramics [35] and that at grain-

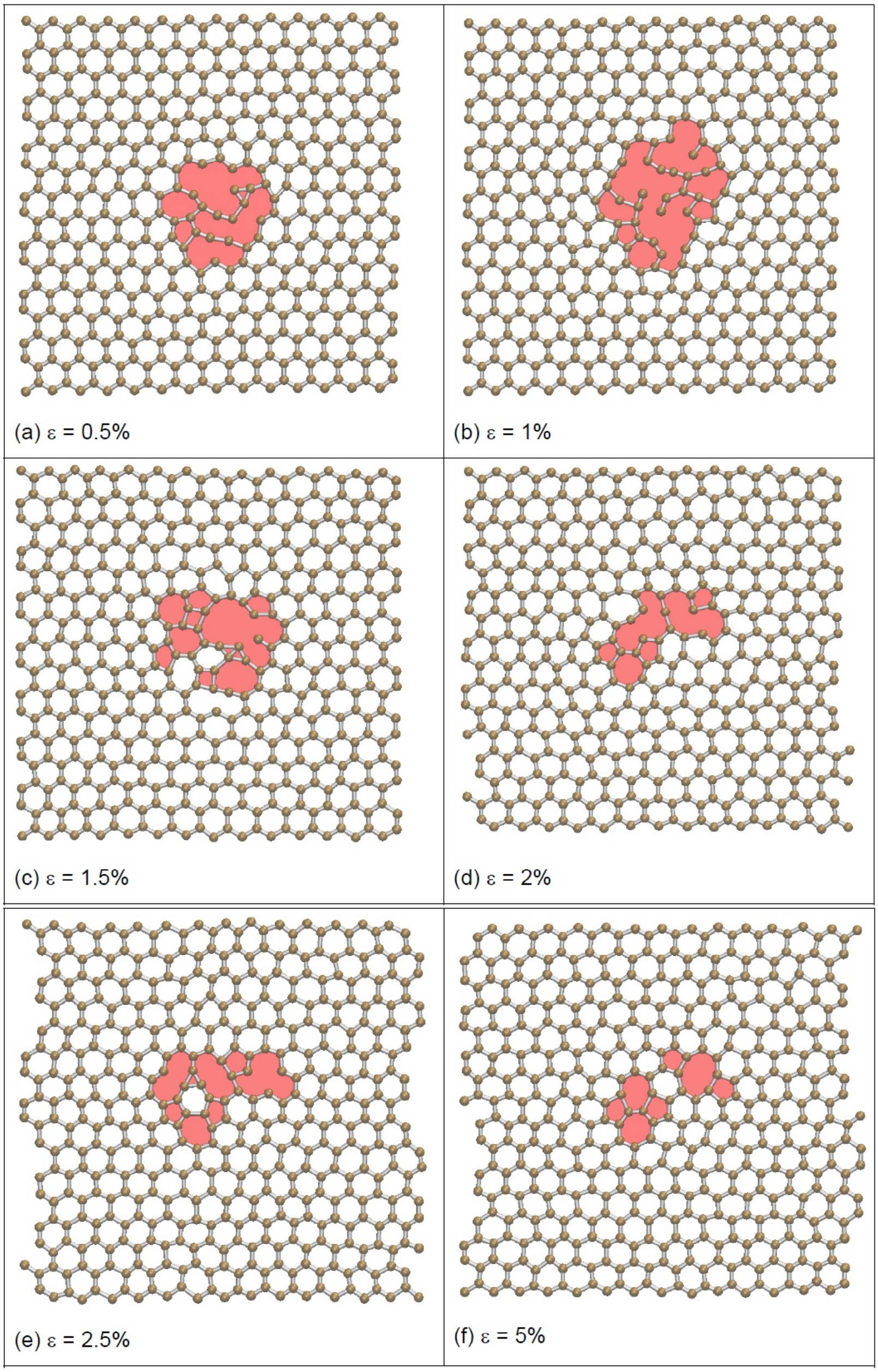

Fig. 2. (Color online) Evolution of graphene sheet with 5-8-5 defect under tensile load at temperature of 2300K. (a) Stress-induced generation of nanoscale amorphous region at the site of the pre-existent 5-8-5 defect at strain $\varepsilon = 0.5\%$. The amorphous region consists of *n*-cells (pink colored cells) of carbon atoms, where $n \neq 6$. (b)-(e) Stress-induced transformations of the amorphous region in graphene at strain $\varepsilon = 1$, 1.5, 2, and 2.5%, respectively. (f) Stress-induced glass-to-crystal transformation occurs in graphene at strain $\varepsilon = 5\%$. As a result, the completely crystalline, but defected structure is formed in the graphene sheet. In doing so, the crystalline graphene sheet contains two defects: a 5-8-5 defect (pink colored configuration consisting of two 5-cells and one 8-cell of carbon atoms) and a Stone-Wales defect (pink colored configuration consisting of two 5-cells and two 7-cells of carbon atoms).

boundary disclinations in poly- and nanocrystalline 3D materials [36]. On the other hand, the process in question resembles evolution of amorphous regions in graphene under irradiation [20-23].

When strain reaches value of $\varepsilon = 5\%$, a reverse glass-to-crystal transformation occurs in the amorphous graphene region (Fig. 2f). As a result, the completely crystalline, but defected structure is formed in the graphene sheet (Fig. 2f). More precisely, the crystalline graphene sheet at $\varepsilon = 5\%$ contains two defects: a 5-8-5 defect (whose orientation is different from that of the initial 5-8-5 defect shown in Fig. 1) and a Stone-Wales defect (Fig. 2f). Further tension of graphene leads to its fast failure.

Thus, our MD simulations have revealed local crystal-to-glass and reverse glass-to-crystal transformations (Fig. 2) in mechanically loaded graphene with a pre-existent 5-8-5 defect at high temperature (2300K) (Fig. 1). Following computer simulations [37], crystal-to-glass transformations induced by mechanical stresses occur in graphene nanoribbons where they are enhanced due to the pronounced edge effects. In contrast, reverse glass-to-crystal transformations were never observed in previous experiments and simulations addressing the structure of graphene during its deformation. The aforesaid is indicative of rather specific conditions of the mechanical test under consideration. We think that high temperature plays the crucial role in initiating the reverse glass-to-crystal transformations (Fig. 2f) in mechanically loaded graphene. In any event, the phenomena of crystal-to-glass and glass-to-crystal transformations in graphene are worth being examined in the future in order to understand its fundamentals.

4. CONCLUDING REMARKS

To summarize, we performed MD simulations (with the AIREBO potential) of deformation processes and structural transformations occurring in graphene sheets containing 5-8-5 defects at temperature of 2300K (Figs. 1 and 2). (Such 5-8-5 defects represent divacancies associated with "pentagon-octagon-pentagon" configurations of carbon atoms in hexagonal crystal lattice of graphene (Fig. 1).) The MD simulations have shown that stress-induced crystal-to-glass and glass-to-crystal transformations occur in a nanoscale region at the initial 5-8-5 defect in graphene (Fig. 2). Crystal-to-glass transformations induced by mechanical stresses and enhanced by the edge effects in graphene have been reported in other simulations [37]. In contrast, reverse glass-to-crystal transformations in graphene are observed in simulations at the first time in our work.

ACKNOWLEDGEMENTS

This work was supported, in part (for ASK), by St. Petersburg State University (research grant 6.37.671.2013) and, in part (for IAO), by the Russian Ministry of Education and Science (Zadanie № 9.1964.2014/K). The simulations were performed at Resource Center "Simulation Center of St. Petersburg State University".

REFERENCES

[1] A.K. Geim and K.S. Novoselov // *Nature Mater.* **6** (2007) 183.
[2] A.K. Geim // *Science* **324** (2009) 1530.
[3] A.H. Castro Nero, F. Guinea, N.M.R. Peres, K.S. Novoselov and A.K. Geim // *Rev. Mod. Phys*. **81** (2009) 109.
[4] A.A. Balandin // *Nature Mater.* **10** (2011) 569.
[5] K.S. Novoselov, V.I. Fal2 ko, L. Colombo, P.R. Gellert, M.G. Schwab and K. Kim // *Nature* **490** (2012) 192.
[6] I.A. Ovid'ko // *Rev. Adv. Mater. Sci.* **34** (2013) 1.
[7] O.V. Yazyev and Y.P. Chen // *Nature Nanotechnol.* **9** (2014) 755.
[8] C. Daniels, A. Horning, A. Phillips, D.V.P. Massote, L. Liang, Z. Bullard, B.G. Sumpter and V. Meunier // *J. Phys.: Condens. Matter* **27** (2015) 373002.
[9] J.-W. Jiang, B.-S. Wang, J.-S. Wang and H.S. Park // *J. Phys.: Condens. Matter* **27** (2015) 083001.
[10] R. Raccichini, A. Varzi, S. Passerini and B. Scorsati // *Nature Mater.* **14** (2015) 271.
[11] T. Kuilla, S. Bhadha, D. Yao, N.H. Kim, S. Bose, J.H. Lee // *Prog. Polymer. Sci.* **35** (2010) 1350.
[12] I.A. Ovid'ko // *Rev. Adv. Mater. Sci.* **34** (2013) 19.
[13] H. Porwal, S. Gresso and M.J. Reece // *Adv. Appl. Ceram*. **112** (2013) 443.
[14] N. Saravanan, R. Rajasekar, S. Mahalakshmi, T.P. Sathishkumar, K.S.K. Sasikumar and S. Sahoo // J. Reinforced Plastics & Composites **33** (2014) 1158.
[15] I.A. Ovid'ko // *Rev. Adv. Mater. Sci.* **38** (2014) 190.
[16] F. Banhart, J. Kotakoski and A.V. Krasheninnikov // *ACS Nano* **5** (2011) 26.

[17] I.A. Ovid'ko // *Rev. Adv. Mater. Sci.* **30** (2012) 201.
[18] L.P. Biro and P. Lambin // *New J. Phys*. **15** (2013) 035024.
[19] J. Lu, Y. Bao, C.L. Su and K.P. Loh // *ACS Nano* **7** (2013) 8357.
[20] J. Kotakoski, A.V. Krasheninnikov, U. Kaiser and J.C. Meyer // *Phys. Rev. Lett.* **106** (2011) 105505.
[21] F.R. Eder, J. Kotakoski, U. Kaiser and J.C. Meyer // *Sci. Rep*. **4** (2014) 4060.
[22] Z. Liang, Z. Xu, T. Yan and F. Ding // *Nanoscale* **6** (2014) 2082.
[23] R. Zhao, J. Zhuang, Z. Liang, T. Yan and F. Ding // *Nanoscale* **7** (2015) 8315.
[24] L. Pelaz, L.A. Marqués and J. Barbolla // *J. Appl. Phys.* **96** (2004) 5947.
[25] A.T. Motta // *J. Nucl. Mater*. **244** (1997) 227.
[26] E. Ma // *Scr. Mater.* **49** (2003) 941.
[27] M. Chen, J.W. McCauley and K.J. Hemker // *Science* **299** (2003) 1563.
[28] I.A. Ovid'ko // *Scr. Mater.* **66** (2012) 402.
[29] K. Lu // *Mater. Sci. Eng. R* **16** (1996) 161.
[30] F. Ye and K. Lu // *Phys. Rev. B* **60** (1999) 7018.
[31] S.J. Stuart, A.B. Tutein and J.A. Harrison // *J. Chem. Phys.* **112** (2000) 6472.
[32] A.S. Kochnev, I.A. Ovid'ko and B.N. Semenov // *Rev. Adv. Mater. Sci.* **37** (2014) 105.
[33] Y.I. Jhon, S.-E. Zhu, J.-H. Ahn and M.S. Jhon // *Carbon* **50** (2012) 3708.
[34] H. Zhao and N. R. Aluru // *J. Appl. Phys*. **108** (2010) 064321.
[35] S.V. Bobylev, I.A. Ovid'ko and A.K. Mukherjee // *Scr. Mater*. **60** (2009) 36.
[36] M.Yu. Gutkin, I.A. Ovid'ko and N.V. Skiba // *Mater. Sci. Eng. A* **339** (2003) 73.
[37] A.S. Kochnev and I.A. Ovid'ko // *Rev. Adv. Mater. Sci.* **43** (2015) 77.